

# Part-based Weighting Aggregation of Deep Convolutional Features for Image Retrieval

Jian Xu  
CASIA

xujian2015@ia.ac.cn

Cunzhao Shi  
CASIA

cunzhao.shi@ia.ac.cn

Chengzuo Qi  
CASIA

qichengzuo2013@ia.ac.cn

Chunheng Wang  
CASIA

chunheng.wang@ia.ac.cn

Baihua Xiao  
CASIA

baihua.xiao@ia.ac.cn

## Abstract

Several recent works have shown that part-based image representation provides state-of-the-art performance for fine-grained categorization. Moreover, it has also been shown that image global representation generated by aggregating deep convolutional features provides excellent performance for image retrieval.

In this paper we propose a novel aggregation method, which utilizes the information of retrieval object parts. The proposed part-based weighting aggregation (PWA) method utilizes the normalized feature maps as part detectors to weight and aggregate the convolutional features. The part detectors which are selected by the unsupervised method highlight the discriminative parts of objects and effectively suppress the noise of background.

We experiment on five public standard datasets for image retrieval. Our unsupervised PWA method outperforms the state-of-the-art approaches based on pre-trained networks and achieves comparable accuracy with the fine-tuned methods. It is worth noting that our unsupervised method is very suitable and effective for the situation where the annotated training dataset is difficult to collect.

## 1. Introduction

Over the past decades, image retrieval has received a sustained attention. Image representations derived by aggregating features such as Scale-Invariant Feature Transform (SIFT) [18] and Convolutional Neural Network (CNN) [17] are shown to be effective for image retrieval [29, 14, 19, 8, 5, 10, 3, 25, 2, 30, 16].

Recently, the performance of CNN-based features aggregation methods [3, 25, 2, 30, 16] rapidly outperforms that of SIFT-based features aggregation methods [29, 14, 19, 8,

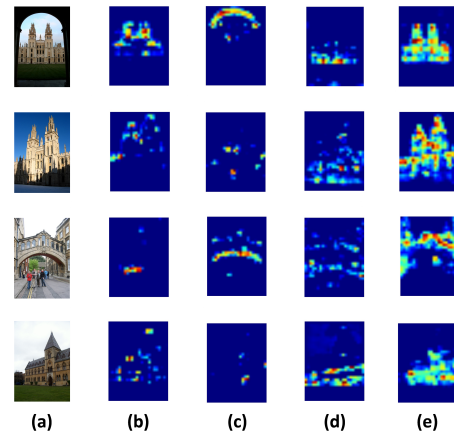


Figure 1. Visualization of the feature maps. (a) Some images in Oxford5K [21]. (b)-(e) The various channels of feature maps in *pool5* layer from pre-trained VGG16 [28]. Each channel of feature maps is activated by different parts or patterns of objects. For example, the (b) 220th feature map is most activated by the sharp shape; the (c) 478th feature map is most activated by the arc shape; the (d) 483th feature map is most activated by the bottom of buildings; the (e) 360th feature map is most activated by the body of buildings.

5, 10]. Some works [26, 6, 3] generate the global representation based on fully connected layer features for image retrieval. After that, convolutional layer features are aggregated to obtain the global representation [25, 2, 30, 16] and achieve better performance. Many recent works [1, 24, 7] re-train the CNNs for image retrieval task by collected landmark buildings datasets. The fine-tuning process significantly improves the adaptation ability for the specific task. However, these methods [1, 24, 7] need to collect the labeled training datasets and the performance of them relies heavily on the collected datasets.

Recently, many works pay attention to the characteristics

and implications of feature maps [17], and they get some primary conclusions. Feature maps [17] activate different parts of objects [9, 35, 34], which are generated by various filters of deep convolutional layers. The filters of convolutional layers can be used as part detectors, and the values of feature maps can be used as detection scores [33, 27]. In [36], the part-based representation is computed by Fisher vector method [19, 20] using selected parts, which are generated by multi-max pooling strategy. As shown in Fig. 1, the discriminative feature maps detect special patterns and semantic parts from retrieval objects. The feature maps contain a wealth of part-based information which is demonstrated to be effective for image retrieval in our experiments. Thus each channel of feature maps can work as a part detector.

However, the previous aggregation methods [26, 6, 3, 25, 2, 30, 16, 1, 24, 7] ignore the information of the object parts. Inspired by the characteristics of feature maps, in this paper we present a novel and simple way of creating powerful image representation via part-based aggregation. The proposed method uses the normalized values of various channels of feature maps as part detectors. Our part-based weighting aggregation (PWA) method improves considerably the state-of-the-art for global representation on standard retrieval datasets, and performs much better than deep global representation for retrieval previously suggested in [25, 2, 30, 16].

Overall, this paper introduces and evaluates a novel part-based aggregation method and investigates the reasons underlying its success. Compared to previous works [26, 6, 3, 25, 2, 30, 16], we demonstrate that the utilization of part-based information leads to a big boost in accuracy. It significantly outperforms the existing methods without fine-tuning on the common retrieval benchmarks. For example, the performance of our PWA method is 79.0% mAP on the Oxford5k dataset, which outperforms the state-of-the-art methods without fine-tuning by 8.2% mAP.

## 2. Related work

In this section, we review several related works from two aspects: aggregated representations and part detectors.

### 2.1. Aggregation methods

The classical approaches to object based image retrieval involve the use of SIFT features [18]. Successful techniques for image retrieval tend to focus on deriving image representations from local descriptors based on aggregation strategy, such as the bag-of-visual-words (BOW) representation [29], BOW with multiple- [12, 13] or soft-assignment [22, 31], locality-constrained liner coding [32], VLAD [14], Fisher vector [19, 20], triangulation embedding [8], Faemb [5] and robust visual descriptor (RVD) aggregation [10].

Several recent aggregation methods consider the use of deep CNN fully connected layer features for image retrieval. Fully connected layer is used as global representation followed by dimensionality reduction [3], and the performance of PCA-compressed representation is better than compact representations computed on traditional SIFT-like features. Simultaneously, [6] proposes the more performant representation based on performing orderless VLAD pooling to aggregate the activations of fully connected layers at multiple scale levels. Related to that, the work [26] reports fairly good retrieval results using sets of multiple sub-patches features of various sizes at different locations that are extracted from fully connected layers of a CNN, without aggregating them into a global representation.

Many recent works derive the visual representation from the activations of convolutional layers. Razavian et al. [25] extend the work [26] to convolutional layers and the use of convolutional layers leads to much better performance. After that, the work [2] introduces a compact global image representation based on sum-pooled convolutional features (SPoC) and further shows that the performance of aggregation methods for deep convolutional features is different from shallow features (e.g., SIFT) because of their higher discriminative ability and different distribution properties. Recent work [30] proposes a compact image representation derived from the convolutional layer activations which encodes multiple image regions of different sizes without the need to re-feed multiple inputs to network. Simultaneously, Kalantidis et al. [16] extend the work of [2] by allowing cross-dimensional weighting.

Finally, many works [1, 24, 7] that fine-tune the pre-trained CNN models for image retrieval demonstrate that the fine-tuned networks can bring a significant improvement for image retrieval task. NetVLAD [1] plugs a trainable generalized VLAD [14] layer into a CNN and re-trains the model for image retrieval and place recognition via the weakly supervised ranking loss, of which the inputs are the feature maps of convolutional layers and the outputs are the global representations. After that, the recent works [24, 7] fine-tune deep CNN features for image retrieval and aggregate the fine-tuned CNN features based on R-MAC [30]. The global representations derived from the activations of the fine-tuned convolutional layers outperform the representations based on pre-trained CNN. However, these methods need to collect the labeled training datasets. The performance of these methods [1, 24, 7] heavily depends on the collected training datasets.

The previous aggregation methods ignore the part-based information of retrieval objects. Inspired by the following works, we propose the PWA method.

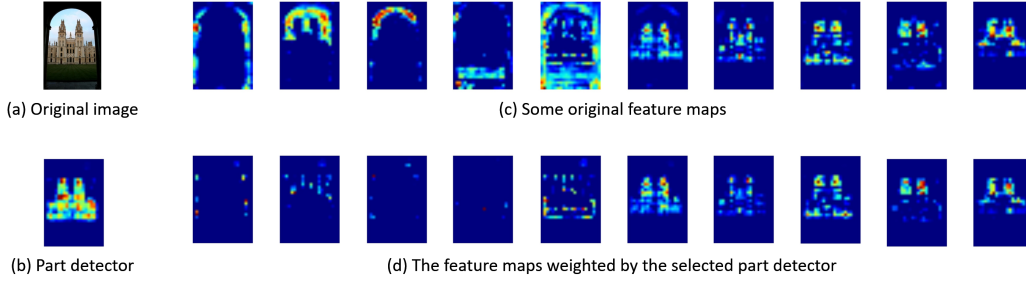


Figure 2. The comparison between the original feature maps and the feature maps weighted by the selected part detector. (a) Original image. (b) The part detector with the largest variances. (c) Some original feature maps. (d) The feature maps weighted by the selected part detector. The pivotal parts of retrieval objects are highlighted (red) and the noise of background is suppressed (blue) by the selected discriminative part detectors.

## 2.2. Part detectors

Recently, some works [9, 35, 34] analyze the meaning of feature maps of CNN. They find that the filters of deep convolutional layers are activated by various semantic content and some distinctive filters can work as part detectors. Zeiler et al. [34] show that some input patterns stimulate the special channels of feature maps of the latter convolutional layers. Kaiming He et al. [9] visualize the feature maps generated by some filters of the *conv*<sub>5</sub> layer from SPP-net [9]. They see that some filters can be activated by the specific semantic content. Recent work [35] picks some distinctive filters which respond to specific patterns significantly and consistently to learn a set of part detectors, and conditionally picks deep filter responses to encode them into the final representation based on Fisher vector [19, 20].

The part-based information is utilized for fine-grained categorization in [33, 27, 36] and the part-based representation provides the state-of-the-art performance. The work [33] uses clustered mid-layer filters to detect parts from region proposals and builds the part-based classifier. The result of [33] shows that the part-based representation is discriminative. Simon et al. [27] propose that the outputs of convolutional layers can be interpreted as detection scores of multiple object part detectors, and select some important outputs from all layers in CNN as parts. In [36], the part-based image representation is generated by aggregating selected parts on several different scales via Fisher vector [19, 20].

Different with above methods, we use the different channels of feature maps of deep convolutional layers as part detectors. Depending on part detectors, we aggregate the CNN features as the global representation.

## 3. Aggregation based on part detectors

In this section, we analyse the characteristics of the responses of deep convolutional layers which can be interpreted as part detectors. Based on the part detectors which activate discriminative parts and patterns of retrieval ob-

jects, we propose a novel and effective PWA method for image retrieval.

In our experiments, we extract features  $f$  from deep convolutional layers by passing an image  $I$  through a pre-trained or fine-tuned deep network, which consist of  $C$  feature maps each having height  $H$  and width  $W$ . Finally, the input image  $I$  is represented by the aggregated  $N \times C$ -dimensional vector that are weighted by the  $N$  selected part detectors.

### 3.1. Part detectors

#### 3.1.1 Motivation

Recent works [9, 35, 34, 27, 36] start to pay attention to the responses of latter convolutional layers. They find that feature maps can be activated by some semantic content [9, 35, 34] and some distinctive feature maps can detect discriminative parts and patterns [27, 36].

To understand the meanings and characteristics of the feature maps, we visualize some images and corresponding typical channels of feature maps in Fig. 1. We select some images in Oxford5K [21] as shown in Fig. 1 (a). In Fig. 1 (b)-(e), We visualize some typical channels of feature maps for the selected images. Each channel of feature maps is activated by different parts or patterns of objects. For example, the 220th feature map (Fig. 1 (b)) of *pool*<sub>5</sub> layers from VGG16 [28] is most activated by the sharp shape; the 478th feature map (Fig. 1 (c)) is most activated by the arc shape; the 483th feature map (Fig. 1 (d)) is most activated by the bottom of buildings; the 360th feature map (Fig. 1 (e)) is most activated by the body of buildings. We can see that distinctive feature maps of convolutional layers respond to some specific patterns. Different feature maps are sensitive to different shapes and positions, and the activations of feature maps highlight different parts and patterns of objects. Some special parts of object are discriminative, for example, the 220th feature maps highlight the spire of buildings. Therefore, feature maps of deep convolutional layer can work as part detectors to pick spe-

cial patterns. The previous CNN-based aggregation methods [26, 6, 3, 25, 2, 30, 16, 24, 7, 1] ignore the part-based information of feature maps. In this paper, we propose a succinct PWA method which combines part-based information with CNN features of convolutional layers.

### 3.1.2 Selection of part detectors

We select the discriminative feature maps as the part detectors by simple unsupervised method. We first calculate the variances  $\{v_1, v_2, \dots, v_c, \dots, v_C\}$  of  $C$ -dimensional vectors  $g_i$  ( $i = 1, 2, \dots, D$ , where  $D$  is the number of images in the training set) computed by sum pooling the features  $f$ . Then we sort the variances  $\{v_1, v_2, \dots, v_C\}$  for  $C$  feature maps. We find that the feature maps with large variances are discriminative, because the responses of them are significantly different among the various objects. We also observe them to be more discriminative by the following experiment. We performed retrieval by PWA but we select (1) 30% random part detectors (2) 30% part detectors with the largest variance. The mAP score for the Oxford5k dataset [21] for (1) is only  $0.775 \pm 0.006$ , which is much small than mAP for (2), 0.790. This verifies that feature maps with large variances are much more discriminative than random feature maps. Remarkably, our simple unsupervised selection method not only boosts the performance but also reduces the cost of computation time.

### 3.1.3 Effects of part detectors

In Fig. 2, we visualize the feature maps which are weighted by the part detector with the largest variances, which is the 360th feature map of *pool5* layer from VGG16 [28]. We compare the original feature maps (in Fig. 2 (c)) with the feature maps weighted by part detectors (in Fig. 2 (d)). The results show that the pivotal parts of retrieval objects are highlighted (red) and the noise of CNN features is suppressed (blue) by the discriminative part detectors. Therefore, The discriminative part detectors activate the corresponding patterns and effectively suppress noise.

To investigate the effects of part detectors in detail, we compare the 512-dimensional representation computed by sum pooling with the representation weighted by the discriminative part detectors in Fig 3. As shown in Fig 3, the selected 220th part detector suppresses the noise of background and activates the sharp shape. The values of feature maps that are activated by background (such as (b) 507th and (c) 155th) are smaller after weighted by the selected part detector. However, the values of the representation responding to patterns or parts that are similar to the selected part detector (such as (d) 53th) still keep large. As a result, the representations weighted by the discriminative part detectors are more prominent and robust. We also conduct

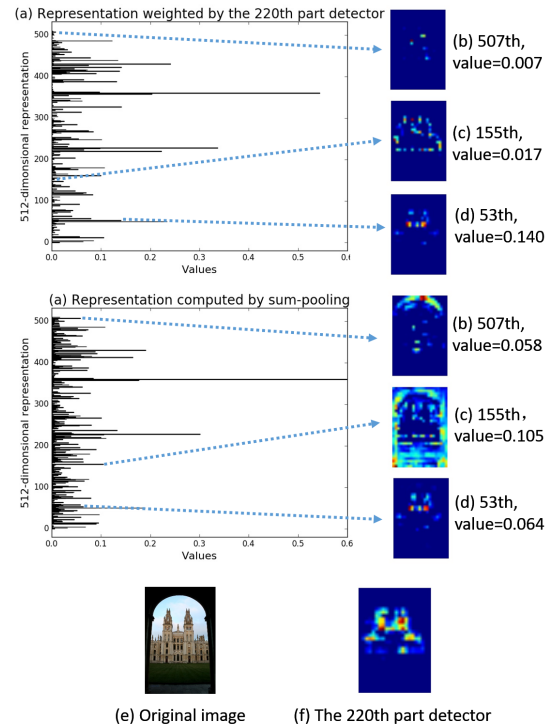


Figure 3. The comparison of the 512-dimensional representations computed by sum pooling and PWA. The values of feature maps that are activated by background (such as (b) 507th and (c) 155th) are smaller after weighted by the selected part detector. However, the values of the representation responding to patterns or parts that are similar to the selected part detector (such as (d) 53th) still keep large. The selected 220th part detector suppresses the noise of background and activates the sharp shape of retrieval object.

an additional experiment to prove that the noise of background can be suppressed by part detectors. We select the  $N$  discriminative part detectors and only use  $N$  channels of feature maps responding to the selected part detectors to generate the (1)  $N \times N$ -dimensional representation rather than (2)  $N \times C$ . The mAP of (1) is nearly same as (2). The result shows that the channels which are not selected are dramatically suppressed by part detectors and almost have no effect on discrimination.

Overall, the feature maps of latter convolutional layers can be interpreted as part detectors. The selected part detectors can suppress the noise of background and highlight the discriminative parts and patterns of objects. We make use of the selected part detectors to weight the activations of convolutional layers and generate the global representation.

## 3.2. PWA design

In this section, we describe the PWA method in detail. We aggregate the feature maps weighted by the selected part detectors and reduce the dimensionality of high-

dimensional representation by PCA.

**Sum pooling weighted by selected part detectors.** The construction of the PWA representation starts with the weighted sum pooling of the  $C \times W \times H$ -dimensional deep convolutional features  $f$  for image  $I$  with height  $H$  and width  $W$ :

$$\psi_n(I) = \sum_{x=1}^W \sum_{y=1}^H w_n(x, y) f(x, y) \quad (1)$$

The coefficients  $w_n$  are the normalized weights as follows, which depend on the activation values  $v_n(x, y)$  in position  $(x, y)$  of the selected part detector  $n$ :

$$w_n(x, y) = \left( \frac{v_n(x, y)}{\left( \sum_{x=1}^W \sum_{y=1}^H v_n(x, y)^\alpha \right)^{1/\alpha}} \right)^{1/\beta} \quad (2)$$

where  $\alpha$  and  $\beta$  are parameters for power normalization and power-scaling respectively.

**Concatenation.**  $N$  selected  $C$ -dimensional representations  $\psi_n(I)$  are obtained from weighted sum pooling process. We aggregate them into the global  $N \times C$ -dimensional representation vector  $\psi(I)$  by concatenating them:

$$\psi(I) = [\psi_1, \psi_2, \dots, \psi_N] \quad (3)$$

where we select the  $N$  part detectors depending on the discrimination of them. The selection based on the values of the variances of different  $C$  channels of feature maps both provides boost in performance and enhances the computation efficiency.

**Post-processing.** We perform  $l_2$ -normalization, PCA compression and whitening on the obtained representation  $\psi(I)$  subsequently and obtain the final  $M$ -dimensional representation  $\psi_{PWA}(I)$ :

$$\psi_{PWA}(I) = \text{diag}(\sigma_1, \sigma_2, \dots, \sigma_M)^{-1} V \frac{\psi(I)}{\|\psi(I)\|_2} \quad (4)$$

where  $V$  is the  $M \times N$  PCA-matrix,  $M$  is the number of the retained dimensionality, and  $\sigma_1, \sigma_2, \dots, \sigma_M$  are the associated singular values.

## 4. Experiments

### 4.1. Datasets

We evaluate the performance of PWA and other aggregation algorithms on five standard datasets for image retrieval.

Oxford Buildings dataset [21] (Oxford5K) contains 5062 images collected from Flickr by searching for particular Oxford landmarks. 55 queries corresponding to 11 buildings

are manually annotated. The performance is measured using mean average precision (mAP) over the 55 queries.

Oxford Buildings dataset+100K [21] (Oxford105K) contains the Oxford Building dataset and additionally 100K distractor images from Flickr.

Paris dataset [23] (Paris6K) contains 6412 photographs from Flickr associated with Paris landmarks. The performance is measured using mean average precision (mAP) over the 55 queries that are manually annotated.

Paris dataset+100K (Paris106K) contains the Paris dataset [23] and additionally 100K distractor images from Flickr [21].

INRIA Holidays dataset [11] (Holidays) is a set of images which mainly contains 1491 personal holidays photos corresponding to 500 groups each having the same scene or object. Query images are the sets of the first image of each group and the correct retrieval results are the other images of the same group. The performance is reported as mean average precision (mAP) over 500 queries. Similarly to [3, 2], we manually fix images in wrong orientation by rotating them by  $\pm 90$  degrees.

### 4.2. Implementation details

We extract deep convolutional features using the pre-trained VGG16 [28] and fine-tuned ResNet101 from the extension of work [7]. In the experiments, Caffe [15] package for CNNs is used. For VGG16 model, we extract convolutional feature maps from the *pool5* layer and the number of channels is  $C=512$ . For ResNet-101 model, we extract convolutional feature maps from the *res5c\_relu* layer and the number of channels is  $C=2048$ . Regarding image size, we keep the original size of the images except for the very large images which are resized to the half size. The parameters for power normalization and power-scaling are set as  $\alpha = 2$  and  $\beta = 2$ , throughout our experiments.

We evaluate the mean average precision (mAP) over the cropped query. To be directly comparable with the related retrieval methods, we learn the PCA and whitening parameters on Oxford5k when testing on Paris6k and vice versa, and we use Oxford5k dataset for whitening on the Holidays.

In our experiment, We use average query expansion (QE) [4] computed by the top 10 query results (except top 2 for Holidays dataset, because the number of images in the same category is two mostly). QE consistently improves the performance on all datasets, although it has a negligible cost.

### 4.3. Impact of the parameters

Our methods only have few parameters to evaluate. The main parameters are the numbers of the selected part detectors and the dimensionality of final representations  $\psi_{PWA}(I)$ .

**Select part detectors.** We use the different channels of feature maps of deep convolutional layers as part detectors. We aggregate the responses of convolutional layers by all the C part detectors as the baseline, which outperforms the state-of-the-art aggregation methods [30, 16]. We also select the discriminative part detectors according to the variances of feature maps.

We show the results of selecting the first N part detectors with the largest variances in Table 1. In this experiment, the final representation  $\psi_{PWA}(I)$  is reduced into 4096 dimensionality by PCA. The variances of feature maps are calculated on Oxford5k dataset, and we select the part detectors according to the values of variances responding to different channels of feature maps.

The part detectors selected depending on the Oxford5k dataset are also suitable for Paris6k. The best performance is archived by selecting N=150 part detectors on both Oxford5k and Paris6k datasets. The selection strategy outperforms above 0.4% than our baseline and reduces the computational cost to about 1/3. The results show that our straightforward unsupervised selection strategy is effective and has good generalization.

Table 1. Performance of different number of selected part detectors. We aggregate the responses of convolutional layers by all the C=512 part detectors as the baseline. The best performance is achieved by selecting N=150 part detectors. Note, the final representation  $\psi_{PWA}(I)$  is reduced into 4096 dimensionality by PCA.

N	Datasets	
	Oxford5k	Paris6k
512	0.785	0.854
450	0.787	0.857
350	0.790	0.857
250	0.787	0.854
150	<b>0.790</b>	<b>0.858</b>
50	0.782	0.852
25	0.788	0.846
10	0.776	0.817

**Dimensionality reduction.** In order to get shorter representations, we compress the  $N \times C$ -dimensional aggregated representation  $\psi(I)$  by PCA and whitening process. Table 2 reports the performance for short vectors of varying dimensionality, M=128 to 4096. We do not reduce the final representation into higher dimensionality because of the limited number of images in Oxford5k and Paris6k datasets. We select N=150 part detectors to aggregate the convolutional features in this experiment.

The results show that the performance boosts gradually with the increase of dimensionality and the best performance is achieved at 4096 dimensionality. The compression leads to the loss of discriminative information. The

previous works [2, 30, 16] aggregate convolutional features as compressed representations with dimensionality under 512, and the compressed representations with lower dimensionality lose more discriminative information. Compared with [2, 30, 16], our PWA methods can generate representations with both low and high dimensionality and achieve better performance.

Table 2. Performance of varying dimensionality, into which the final representation is reduced. The representation is reduced by PCA and whitening. The best performance is achieved at 4096 dimensionality. Note, we select 150 part detectors to aggregate the convolutional features.

M	Datasets	
	Oxford5k	Paris6k
128	0.642	0.642
256	0.687	0.775
512	0.722	0.809
1024	0.755	0.832
2048	0.776	0.845
4096	<b>0.790</b>	<b>0.858</b>

## 4.4. Comparison with the state-of-the-art

### 4.4.1 Methods without fine-tuning

In the first part of Table 3, we compare our PWA method using pre-trained VGG16 [28] with the current state-of-the-art methods without fine-tuning, which employ global representations of images. The results show that our method significantly outperform them on all 5 standard retrieval datasets, and especially the gain is more than 8.2% in mAP for Oxford5k and Oxford105k. This demonstrates that the part-based weighting is effective and our PWA representations are discriminative. Our 512-dimensional PWA representation is comparable with the previous state-of-the-art, and its results are only lower than R-MAC [30] on Paris6k and Paris106k. The PWA representation with higher dimensionality (such as 1024, 2048 and 4096) consistently outperform all of them on all datasets.

We compare with other methods that contain query expansion (QE) with our approach that contains query expansion process in the second part of Table 3. Query expansion improves the performance at low extra cost. Our PWA+QE method performs better than the related works [30, 16] on every dataset, though the approximate max pooling localization (AML) process [30] requires a costly verification stage and the extra memory storage.

### 4.4.2 Methods with fine-tuning

We also compare our method with the current state-of-the-art methods containing fine-tuning process (e.g., [1, 24])

Table 3. Accuracy comparison with the state-of-the-art methods without fine-tuning. We compare our PWA+QE with other methods followed by query expansion at the bottom of table. Part-based weighting aggregation (PWA) consistently outperforms the state-of-the-art aggregation methods.

Method	Dimensionality	Datasets				
		Oxford5k	Paris6k	Oxford105k	Paris106k	Holidays
Triangulation embedding [8]	1024	56.0	—	50.2	—	72.0
Triangulation embedding [8]	8k	67.6	—	61.1	—	77.1
FAemb [5]	8k	66.7	—	—	—	76.2
FAemb [5]	16k	70.9	—	—	—	78.7
RVD-W [10]	8k	66.8	—	64.0	—	76.5
RVD-W [10]	16k	68.9	—	66.0	—	78.8
Razavian et al. [25]	512	46.2	67.4	—	—	74.6
Neural Codes [3]	512	43.5	—	39.2	—	—
SPoC [2]	256	53.1	—	50.1	—	80.2
R-MAC [30]	512	66.9	83.0	61.6	75.7	—
CroW [16]	512	70.8	79.7	65.3	72.2	85.1
Previous state-of-the-art		70.8	83.0	65.3	75.7	85.1
PWA	512	72.2	80.9	66.2	73.8	87.3
PWA	1024	75.5	83.2	69.3	76.1	87.9
PWA	2048	77.6	84.5	71.1	78.2	88.2
PWA	4096	<b>79.0</b>	<b>85.8</b>	<b>73.6</b>	<b>79.1</b>	<b>88.3</b>
CroW+QE [16]	512	74.9	84.8	70.6	79.4	—
R-MAC+AML+QE [30]	512	77.3	86.5	73.2	79.8	—
PWA+QE	4096	<b>81.4</b>	<b>88.9</b>	<b>77.4</b>	<b>83.5</b>	<b>89.0</b>

Table 4. Accuracy comparison with the state-of-the-art methods with fine-tuning. Without the end-to-end training, we achieve the comparable performance with them.

Method	Dimensionality	Datasets		
		Oxford5k	Paris6k	Holidays
NetVLAD [1]	4096	71.6	79.7	87.5
Radenoviac et al. [24]	512	79.7	83.8	82.5
Extension of Gordo et al. [7]	2048	84.1	<b>93.6</b>	<b>94.0</b>
Previous state-of-the-art		84.1	93.6	94.0
PWA	4096	<b>84.8</b>	92.0	89.2

and the extension of work [7]) in Table 4. While our proposed PWA method does not need the end-to-end training, it achieves the comparable performance with them. In this experiment, we compare the proposed method with the result of extension of work [7] that does not contain multi-resolution process which bring extra computational cost at feature extract time (approximately three times the cost for three resolutions). We use convolutional layers features of fine-tuned ResNet101 from the extension of work [7].

The scores of PWA are only lower than that of the extension of work [7] on Paris6k and Holidays. In the extension of work [7], the PCA is replaced by the shifting and fully connected layers. The optimal weights for them are learned

end-to-end. Compared with it, the strategy of dimensionality reduction and whitening in our method is unsupervised. In Table 5, we compare our PWA method with the extension of work [7] which not containing shifting and fully connected layers. As shown in Table 5, our PWA method performs better than the network without shifting and fully connected layers [7]. The results demonstrate that the supervised shifting and fully connected layers are important for the performance of this fine-tuned network, while we only use the convolutional layers of it. We will explore the more effective method to reduce the dimensionality of representation in the future work.

The effect of fine-tuning is dependent on the collected



Table 5. Accuracy comparison with the extension of the work [7] without shifting and fully connected layers. Our PWA method significantly improves the performance.

Method	Dimensionality	Datasets		
		Oxford5k	Paris6k	Holidays
Extension of Gordo et al. [7] w/o Shift+FC	2048	78.7	89.7	89.1
PWA	4096	<b>84.8</b>	<b>92.0</b>	<b>89.2</b>

training set. The images in Oxford5k and Paris6k datasets are almost landmarks. However most images in Holidays dataset are photographs of landscapes. The networks [24, 7] that are fine-tuned by the landmark buildings dataset significantly improve the performance on Oxford5k and Paris6k datasets but only help little on the performance on Holidays dataset. However, our PWA method can make better use of the features extracted from both pre-trained and fine-tuned CNN model to represent the images and does not need the further re-training. Considering the fact that the annotated training dataset is difficult to collect, we can not fine-tune the model for some particular task. Our method is very suitable for this condition, which selects part detectors by unsupervised strategy and aggregates discriminative part-based convolutional features to represent the images. Our PWA method retains more discriminative information of the retrieval object parts and effectively suppress the noise of background, and can better utilize the convolutional features extracted from both pre-trained and fine-tuned CNN models.

## 5. Conclusion

In this paper, we propose a novel PWA method for image retrieval. The key characteristic of our method is that it uses discriminative part detectors selected without supervision to weight and aggregate the deep convolutional features extracted from pre-trained or fine-tuned CNN models. The results show that our PWA method can suppress the noise of background and highlight the discriminative parts and patterns of retrieval objects.

Experiments on five standard retrieval datasets demonstrate that our unsupervised approach outperforms the previous state-of-the-art aggregation methods without fine-tuning and achieve the comparable performance to the fine-tuned methods. It is worth noting that our unsupervised PWA method is very suitable and effective for the situation where the annotated training dataset is difficult to collect.

In our future work, we plan to cluster the initial part detectors to select some more discriminative part detectors and reduce the number of selected part detectors. In addition, the end-to-end dimensionality reduction strategy can be considered to improve the performance.

## References

- [1] R. Arandjelovic, P. Gronat, A. Torii, T. Pajdla, and J. Sivic. Netvlad: Cnn architecture for weakly supervised place recognition. In *Proceedings of the IEEE Conference on Computer Vision and Pattern Recognition*, pages 5297–5307, 2016.
- [2] A. Babenko and V. Lempitsky. Aggregating local deep features for image retrieval. In *Proceedings of the IEEE international conference on computer vision*, pages 1269–1277, 2015.
- [3] A. Babenko, A. Slesarev, A. Chigorin, and V. Lempitsky. Neural codes for image retrieval. In *European conference on computer vision*, pages 584–599. Springer, 2014.
- [4] O. Chum, J. Philbin, J. Sivic, M. Isard, and A. Zisserman. Total recall: Automatic query expansion with a generative feature model for object retrieval. In *Computer Vision, 2007. ICCV 2007. IEEE 11th International Conference on*, pages 1–8. IEEE, 2007.
- [5] T.-T. Do, Q. D. Tran, and N.-M. Cheung. Faemb: a function approximation-based embedding method for image retrieval. In *Proceedings of the IEEE Conference on Computer Vision and Pattern Recognition*, pages 3556–3564, 2015.
- [6] Y. Gong, L. Wang, R. Guo, and S. Lazebnik. Multi-scale orderless pooling of deep convolutional activation features. In *European conference on computer vision*, pages 392–407. Springer, 2014.
- [7] A. Gordo, J. Almazan, J. Revaud, and D. Larlus. Deep image retrieval: Learning global representations for image search. In *European Conference on Computer Vision*, pages 241–257. Springer, 2016.
- [8] H. Gou and A. Zisserman. Triangulation embedding and democratic aggregation for image search. In *Computer Vision and Pattern Recognition*, pages 3310–3317, 2014.
- [9] K. He, X. Zhang, S. Ren, and J. Sun. Spatial pyramid pooling in deep convolutional networks for visual recognition. In *European Conference on Computer Vision*, pages 346–361. Springer, 2014.
- [10] S. S. Husain and M. Bober. Improving large-scale image retrieval through robust aggregation of local descriptors. *IEEE Transactions on Pattern Analysis and Machine Intelligence*, 2016.
- [11] H. Jegou, M. Douze, and C. Schmid. Hamming embedding and weak geometric consistency for large scale image search. In *European conference on computer vision*, pages 304–317. Springer, 2008.



- [12] H. Jégou, M. Douze, and C. Schmid. Improving bag-of-features for large scale image search. *International journal of computer vision*, 87(3):316–336, 2010.
- [13] H. Jégou, C. Schmid, H. Harzallah, and J. Verbeek. Accurate image search using the contextual dissimilarity measure. *IEEE Transactions on Pattern Analysis and Machine Intelligence*, 32(1):2–11, 2010.
- [14] H. Jégou, F. Perronnin, M. Douze, J. Sánchez, P. Pérez, and C. Schmid. Aggregating local image descriptors into compact codes. *IEEE Transactions on Pattern Analysis and Machine Intelligence*, 34(9):1704–16, 2012.
- [15] Y. Jia, E. Shelhamer, J. Donahue, S. Karayev, J. Long, R. Girshick, S. Guadarrama, and T. Darrell. Caffe: Convolutional architecture for fast feature embedding. In *Proceedings of the 22nd ACM international conference on Multimedia*, pages 675–678. ACM, 2014.
- [16] Y. Kalantidis, C. Mellina, and S. Osindero. Cross-dimensional weighting for aggregated deep convolutional features. In *European Conference on Computer Vision*, pages 685–701. Springer, 2016.
- [17] Y. LeCun, B. Boser, J. S. Denker, D. Henderson, R. E. Howard, W. Hubbard, and L. D. Jackel. Backpropagation applied to handwritten zip code recognition. *Neural computation*, 1(4):541–551, 1989.
- [18] D. G. Lowe. Distinctive image features from scale-invariant keypoints. *International Journal of Computer Vision*, 60(60):91–110, 2004.
- [19] F. Perronnin and C. Dance. Fisher kernels on visual vocabularies for image categorization. In *IEEE Conference on Computer Vision and Pattern Recognition*, pages 1–8, 2007.
- [20] F. Perronnin, J. Nchez, and T. Mensink. Improving the fisher kernel for large-scale image classification. In *Computer Vision - ECCV 2010, European Conference on Computer Vision, Heraklion, Crete, Greece, September 5-11, 2010, Proceedings*, pages 143–156, 2010.
- [21] J. Philbin, O. Chum, M. Isard, J. Sivic, and A. Zisserman. Object retrieval with large vocabularies and fast spatial matching. In *Computer Vision and Pattern Recognition, 2007. CVPR’07. IEEE Conference on*, pages 1–8. IEEE, 2007.
- [22] J. Philbin, O. Chum, M. Isard, J. Sivic, and A. Zisserman. Lost in quantization: Improving particular object retrieval in large scale image databases. In *Computer Vision and Pattern Recognition, 2008. CVPR 2008. IEEE Conference on*, pages 1–8, 2008.
- [23] J. Philbin, O. Chum, M. Isard, J. Sivic, and A. Zisserman. Lost in quantization: Improving particular object retrieval in large scale image databases. In *Computer Vision and Pattern Recognition, 2008. CVPR 2008. IEEE Conference on*, pages 1–8. IEEE, 2008.
- [24] F. Radenovic, G. Toliás, and O. Chum. Cnn image retrieval learns from bow: Unsupervised fine-tuning with hard examples. In *European Conference on Computer Vision*, pages 3–20. Springer, 2016.
- [25] A. S. Razavian, J. Sullivan, S. Carlsson, and A. Maki. Visual instance retrieval with deep convolutional networks. *IEEE Transactions on Media Technology and Applications*, 4(3):251–258, 2016.
- [26] A. Sharif Razavian, H. Azizpour, J. Sullivan, and S. Carlsson. Cnn features off-the-shelf: an astounding baseline for recognition. In *Proceedings of the IEEE Conference on Computer Vision and Pattern Recognition Workshops*, pages 806–813, 2014.
- [27] M. Simon and E. Rodner. Neural activation constellations: Unsupervised part model discovery with convolutional networks. In *Proceedings of the IEEE International Conference on Computer Vision*, pages 1143–1151, 2015.
- [28] K. Simonyan and A. Zisserman. Very deep convolutional networks for large-scale image recognition. *ICLR 2015*, 2015.
- [29] J. Sivic and A. Zisserman. Video google: A text retrieval approach to object matching in videos. In *IEEE International Conference on Computer Vision*, page 1470, 2003.
- [30] G. Toliás, R. Sicić, and H. Jégou. Particular object retrieval with integral max-pooling of cnn activations. *ICLR*, 2016.
- [31] J. C. van Gemert, C. J. Veenman, A. W. Smeulders, and J. M. Geusebroek. Visual word ambiguity. *IEEE Transactions on Pattern Analysis and Machine Intelligence*, 32(7):1271–83, 2010.
- [32] J. Wang, J. Yang, K. Yu, F. Lv, T. Huang, and Y. Gong. Locality-constrained linear coding for image classification. In *Computer Vision and Pattern Recognition (CVPR), 2010 IEEE Conference on*, pages 3360–3367. IEEE, 2010.
- [33] T. Xiao, Y. Xu, K. Yang, J. Zhang, Y. Peng, and Z. Zhang. The application of two-level attention models in deep convolutional neural network for fine-grained image classification. In *Proceedings of the IEEE Conference on Computer Vision and Pattern Recognition*, pages 842–850, 2015.
- [34] M. D. Zeiler and R. Fergus. Visualizing and understanding convolutional networks. In *European conference on computer vision*, pages 818–833. Springer, 2014.
- [35] X. Zhang, H. Xiong, W. Zhou, W. Lin, and Q. Tian. Picking deep filter responses for fine-grained image recognition. In *Proceedings of the IEEE Conference on Computer Vision and Pattern Recognition*, pages 1134–1142, 2016.
- [36] Y. Zhang, X.-S. Wei, J. Wu, J. Cai, J. Lu, V.-A. Nguyen, and M. N. Do. Weakly supervised fine-grained categorization with part-based image representation. *IEEE Transactions on Image Processing*, 25(4):1713–1725, 2016.